



Published in final edited form as:

Kidney Int. 2015 January ; 87(1): 95–108. doi:10.1038/ki.2014.217.

High mobility group box 1 is a novel deacetylation target of Sirtuin1

May M. Rabadi, PhD¹, Sandhya Xavier, PhD¹, Radovan Vasko, MD, PhD¹, Kavneet Kaur, MD¹, Michael S. Goligorsky, MD, PhD^{1,2,3}, and Brian B. Ratliff, PhD^{1,3}

¹Department of Medicine, New York Medical College, Valhalla, NY 10595

²Department of Pharmacology, New York Medical College, Valhalla, NY 10595

³Department of Physiology, New York Medical College, Valhalla, NY 10595

Abstract

High mobility group box 1 (HMGB1) undergoes acetylation, nuclear-to-cytoplasmic translocation and release from stressed kidneys, unleashing a signaling cascade of events leading to systemic inflammation. Here we tested whether the deacetylase activity of Sirtuin1 (SIRT1) participates in regulating nuclear retention of HMGB1 to ultimately modulate damage signaling initiated by HMGB1 secretion during stress. When immunoprecipitated acetylated HMGB1 was incubated with SIRT1, HMGB1 acetylation decreased by 57%. Proteomic analysis showed that SIRT1 deacetylates HMGB1 at four lysine residues (55, 88, 90 and 177) within the pro-inflammatory and nuclear localization signal domains of HMGB1. Genetic ablation or pharmacological inhibition of SIRT1 in endothelial cells increased HMGB1 acetylation and translocation. *In vivo*, deletion of SIRT1 reduced nuclear HMGB1 while increasing its acetylation and release into circulation during basal and ischemic conditions causing increased renal damage. Conversely, resveratrol pretreatment led to decreased HMGB1 acetylation, its nuclear retention, decreased systemic release and reduced tubular damage. Thus, a vicious cycle is set into motion in which the inflammation-induced repression of SIRT1 disables deacetylation of HMGB1, facilitates its nuclear-to-cytoplasmic translocation and systemic release, thereby maintaining inflammation.

Introduction

High-mobility group box 1 protein (HMGB1) is a ubiquitous 215-amino acid nuclear protein that binds to DNA and promotes its bending, while maintaining genome stability, DNA processing and repair, and controlling autophagy and autophagic clearance of defective mitochondria by regulating the transcription of heat shock protein 27.¹ In addition to these intracellular homeostatic functions and regulation of energy metabolism, HMGB1 can be released from necrotic and non-lethally damaged cells into the extracellular milieu where it behaves as a pro-inflammatory cytokine.² While in the case of necrosis the passive

Users may view, print, copy, and download text and data-mine the content in such documents, for the purposes of academic research, subject always to the full Conditions of use:http://www.nature.com/authors/editorial_policies/license.html#terms

Correspondence/reprint requests: BB Ratliff (Ratliffbb@gmail.com), 15 Dana Rd, New York Medical College – BSB C-06, Valhalla, NY 10595, Phone: 914-594-4733, Fax: 914-594-4732.

Disclosure: All the authors declared no competing interests.

liberation of HMGB1 appears to represent a consequence of nucleorrhexis, much interest has been placed on the process of HMGB1 translocation across the nuclear and plasma membranes of non-lethally stressed cells. It has been demonstrated that nuclear-to-cytoplasmic translocation of HMGB1 results in its accumulation in secretory endolysosomes.³ HMGB1 released locally and systemically exerts an array of actions typical of a damage-associated molecular pattern (DAMP) signal molecule, such as activation of monocytes and dendritic cells, disruption of epithelial and endothelial barriers, cytokine production, mobilization and differentiation of stem cells, and facilitation of tissue repair and regeneration.⁴ This panoply of actions mediated via 5 different receptors, the main of them being Toll-like receptor 4 (TLR4) and receptor for advanced glycosylation endproducts (RAGE), fully justifies the search for molecular mechanisms of HMGB1 translocation.

Posttranslational modifications play a role in HMGB1 localization. HMGB1 phosphorylation has been implicated in its nuclear-to-cytoplasmic translocation.⁵ Hyperphosphorylation on serine residues within two nuclear localization signals (NLS) of HMGB1 in monocytes was found to be responsible for the blockade of its nuclear import and facilitation of cytoplasmic translocation. On the other hand, hyperacetylation of HMGB1 affects its DNA binding⁶ and redirects it towards the cytoplasm⁷ and the secretory pathway with the assistance of an exportin, chromosome region maintenance 1 (CRM1). Recent studies on HMGB1 release from hepatocytes and neuronal cells during ischemia-reperfusion injury (IRI) not only reconfirmed the role of acetylation in HMGB1 export, but also identified the decreased activity of histone deacetylases 1, 4 and 5 (HDAC1, HDAC4 and HDAC5) as critical for HMGB1 hyperacetylation.^{8,9}

It is intriguing that another group of enzymes with deacetylase activity, sirtuins and especially NAD-dependent deacetylase Sirtuin 1 (SIRT1), is a predominantly nuclear protein which can shuttle to the cytoplasm under conditions of cell stress.¹⁰ Such a parallel trafficking of SIRT1 and HMGB1 evokes a possibility of their concomitant interaction and a role for SIRT1 in HMGB1 deacetylation and subsequent nuclear retention. Therefore, the goal of this study was to investigate this possibility.

Results

Release of HMGB1 into the systemic circulation has been observed during onset of acute injury of the heart,¹¹ brain¹² and the kidney.^{13,14} To ascertain the site of its release, we previously measured arterio-venous differences in HMGB1 levels after an IRI model of acute kidney injury (AKI). We observed HMGB1 levels in the blood collected from the renal vein exceeded those in the arterial blood already 1 hour after reperfusion and persisted for the following 3-24 hours.¹⁵ This dynamics of HMGB1 release from the acutely injured kidney argues that a) the kidney is the source of HMGB1 release and b) that this process is a result of the translocation from the existing cellular nuclear pool rather than *de novo* synthesis. These previous findings prompted us to examine the process of HMGB1 translocation during acute kidney and cellular injury.

In vitro endothelial cell studies using SIRT1 inhibitor

In stressed cultured endothelial cells, HMGB1 nuclear-to-cytoplasmic translocation was increased and associated with the concomitantly elevated proportion of the acetylated form that also increased in the cytoplasm 4 hours after LPS treatment, as measured by Western blot (Fig. 1A&B) and imaged at 24 hours using immunocytochemistry (Fig. 2). When an inhibitor of SIRT1 (SIRT1 Inhibitor III) was administered to cultured endothelial cells in the absence of stressor, both HMGB1 acetylation and nuclear-to-cytoplasmic translocation were significantly augmented. This observation suggests nuclear SIRT1 interacts with HMGB1 and plays a role in its nuclear retention. However, when SIRT1 inhibitor was added to cells in conjunction with the stressor (LPS), acetylation and translocation of HMGB1 were not augmented. It's expected that the lack of an additive effect occurs because LPS stress already inhibits SIRT1 and therefore cancels any further effect of the SIRT1 inhibitor.

In parallel, cultured endothelial cells transfected with HMGB1-GFP constructs and imaged in real-time using intravital microscopy showed nuclear-to-cytoplasmic translocation when treated with SIRT1 inhibitor, as judged by increased fluorescence intensity in the cytoplasmic compartment (Fig. 3A&B). Administration of LPS for 24 hours also promoted HMGB1 translocation into the cytoplasm, similar to reports by others.^{16,17} LPS and SIRT1 inhibitor co-administration did not further enhance HMGB1 in the cytosol. In contrast to what we observed after 4 hours of LPS and/or SIRT1 inhibitor administration, both LPS and SIRT1 inhibitor treatment for 24 hours increased HMGB1-GFP fluorescence in the nucleus, suggesting enhanced synthesis of the protein at this later time point (which is supported by reports from other laboratories who observed enhanced HMGB1 expression in macrophages and skeletal muscle cells treated with LPS >12 hours).^{18,19}

SIRT1 specific deacetylation of HMGB1

To further examine the possibility of SIRT1 targeting HMGB1 for deacetylation, we co-incubated acetylated HMGB1 (immunoprecipitated from whole kidney lysates obtained 1 hour after 30 minutes of IRI) with rSIRT1 and its required co-factors, NAD⁺ and Mg²⁺ (Fig. 4). The data demonstrated the acetylated fraction was decreased by 57% within 60 minutes of co-incubation with rSIRT1, thus confirming *in vitro* the possibility that HMGB1 may represent a substrate for SIRT1 deacetylation. When the required SIRT1 cofactor NAD⁺ was omitted from the assay or when SIRT1 was heat inactivated, HMGB1 remained acetylated, thereby confirming SIRT1 specificity for HMGB1.

Further analysis by mass spectrometry of the HMGB1 residues that were deacetylated by SIRT1 showed that the amplitude of specific acetylated lysine peaks at 126 m/z on the MS/MS spectra were significantly reduced after SIRT1 treatment (Fig. 5). The 126 m/z peak represents acetylated lysine residues within the indicated HMGB1 proteolytic fragment (as labeled on each of the MS/MS spectra), therefore reduction in the intensity of the 126 m/z peak indicates reduced acetylation of the represented lysine residue(s) within that fragment. SIRT1 treatment caused reduction in representative acetylation peaks for 4 lysine residues within HMGB1 including Lys55 (near the vital Cys45 residue), Lys88 and Lys90 (in the pro-inflammatory cytokine domain) and Lys177 (in the NLS-2) (Figs. 6A&B). Imaging SIRT1 deacetylated lysines 55, 88 and 90 within the 3-D protein structure of HMGB1

illustrates their location in relation to multiple adjacent hydrophobic residues (Fig. 6C), which enhances their potential for deacetylation by SIRT1.²⁰ Lys55 is adjacent to Met52, Ala54 and Trp49 (Fig. 6D); Lys88 and Lys90 are adjacent to Phe89, Pro92 Ala94 and Pro 95 (Fig. 6E); and Lys177 is positioned next to Ala171, Val175, Val176, Ala178 and Val179. The 3-D protein structure for HMGB1 is currently not available for Lys177.

SIRT1 endothelial *-/-* studies

Since the viability of SIRT1-null mice is poor, we established a viable colony of endothelial SIRT1-deficient mice using the Cre/lox-conditional system associated with the endothelial specific Tie-2 promoter.²¹ These mice are phenotypically indistinguishable from the SIRT1 Flox/Flox (wild-type) littermates and thrive normally. Primary cultures of aortic endothelial cells from SIRT1 endothelial *-/-* mice showed that under basal conditions the proportion of nuclear HMGB1 was decreased with the concomitant increase in its cytoplasmic content as compared to endothelial cells obtained from SIRT1 Flox/Flox mice (Fig. 7A&B). Stimulation with a non-lethal dose of LPS resulted in a surge of cytoplasmic HMGB1 within 4 hours in cells obtained from all animals. The data indicate that SIRT1 activity is required for the maintenance of the nuclear localization of HMGB1, but its translocation in response to endotoxin stimulation is independent of SIRT1. Alternatively, if SIRT1 undergoes a similar-to-HMGB1 translocation after exposure to LPS, this might indicate the loss of nuclear deacetylase occurs even in SIRT1 Flox/Flox cells and thus governs HMGB1 translocation. Importantly, our lab has previously reported cellular stress depletes nuclear SIRT1 activity in endothelial cells,²¹ further suggesting HMGB1 translocation during injury is enhanced because of the loss of SIRT1 deacetylation activity.

Under basal conditions, SIRT1 endothelial *-/-* animals demonstrated a trend of reduced nuclear HMGB1 and enhanced fraction of acetylated HMGB1 in the nucleus and systemic circulation (Fig. 8A-D). One hour after a 30 minute episode of bilateral renal IRI, HMGB1 in the nuclear compartment decreased in the SIRT1 Flox/Flox and SIRT1 endothelial *-/-* animals, although the reduction of nuclear HMGB1 was significantly enhanced in the SIRT1 endothelial *-/-* animals lacking SIRT1 deacetylase activity. Reduced nuclear HMGB1 was associated with an increase in the proportion of acetylated HMGB1 in the nucleus, an effect that was augmented in SIRT1 endothelial *-/-* mice. Release of HMGB1 into the circulation was more robust in SIRT1 endothelial *-/-* mice, as was the proportion of circulating acetylated HMGB1, compared to SIRT1 Flox/Flox mice. Hence, results obtained from stressed SIRT1 endothelial *-/-* mice demonstrate elevated HMGB1 translocation and release during basal conditions and even more so during renal injury. Enhanced HMGB1 release is associated with amplified HMGB1 acetylation during the abrogation of SIRT1 activity, evidence that normal SIRT1 deacetylase activity mediates nuclear HMGB1 retention.

Having demonstrated the role of SIRT1 deacetylation in HMGB1 nuclear-to-cytoplasmic translocation, the corollary of this finding would predict that by priming the cells with SIRT1 prior to renal IRI, post-ischemic HMGB1 translocation could be alleviated. Therefore, we pretreated FVB/NJ mice with resveratrol for 7 days prior to renal ischemia. Cell fractionation of whole kidneys from untreated mice demonstrated that the nuclear localization of HMGB1 was significantly decreased 1 hour post-ischemia, whereas its

cytoplasmic abundance of acetylated HMGB1 had increased (Fig. 9). In contrast, pretreatment with resveratrol drastically blunted nuclear-to-cytoplasmic HMGB1 translocation and reduced levels of acetylated HMGB1 observed in the cytoplasm. The effects of resveratrol pretreatment were even more pronounced when analyzing HMGB1 in the plasma. Renal IRI led to a robust increase in circulating total and acetylated HMGB1; however, resveratrol significantly attenuated levels of both in the plasma, as well as reducing HMGB1 urinary excretion.

Resveratrol pretreatment consistently resulted in increased nuclear HMGB1 retention (Fig. 10A) and reduced systemic HMGB1 plasma levels (Fig. 10B) one hour after bilateral IRI (the latter more pronounced in SIRT1 Flox/Flox than SIRT1 endothelial $-/-$ mice) despite the fact that no statistically significant differences in BUN levels were detected between experimental groups (Fig. 10C). Histological analysis revealed that SIRT1 endothelial ablation led to enhanced renal damage 24 hours post-ischemia (Fig. 11A&B). While resveratrol significantly reduced necrosis in SIRT1 endothelial $-/-$ kidneys, pretreatment was ineffective in reducing brush border loss, cast formation and leukocyte infiltration at this time point. Interestingly, 5 days after unilateral renal IRI, both the ischemic and the contralateral control kidneys of SIRT1 endothelial $-/-$ mice showed worse damage than that observed in SIRT1 Flox/Flox mice, including enhanced necrosis, brush border loss, tubular dilation and fibrosis (Fig. 12A&B).

Discussion

Endothelial cell specific ablation of SIRT1 results in a more severe course of AKI and cardiovascular disease during aging and after vascular stress or pre-existing disease.²¹⁻²³ Due to its suppression of inflammation and premature senescence, we sought to examine the influence of SIRT1 on the pro-damage alarmin HMGB1 in the endothelium during AKI. Data presented herein establish a functional link between the deacetylase SIRT1 and posttranslational modification of HMGB1. Several lines of evidence support this notion. Firstly, nearly half of hyperacetylated HMGB1 is deacetylated within 1 hour *in vitro* by added SIRT1. MS/MS analysis of SIRT1-targeted lysine residues revealed four lysine residues at positions 44, 88, 90 and 177. Secondly, inhibition of SIRT1 in cultured endothelial cells results in the increased proportion of a) acetylated HMGB1 and b) enhanced nuclear-to-cytoplasmic translocation under basal conditions. Thirdly, endothelial cells obtained from mice lacking SIRT1 in the vascular endothelium show the tendency to express higher proportion of HMGB1 in the cytoplasm. Fourthly, in whole animal experiments, mice lacking SIRT1 in the vascular endothelium demonstrated reduced nuclear HMGB1 and an exaggerated surge in HMGB1 acetylation and release into the circulation (as compared to SIRT1 Flox/Flox animals) during basal and ischemic stress. Finally, pretreatment of SIRT1 Flox/Flox mice with SIRT1 activator, resveratrol, reduces the extent of acetylation and improves nuclear retention of HMGB1 after imposition of ischemic insult. At the same time, the post-ischemic surge of HMGB1 in the plasma of these mice is blunted after pretreatment with resveratrol. These findings not only are consistent with the earlier observations linking the state of HMGB1 acetylation with its nuclear-to-cytoplasmic translocation, but also identify SIRT1 as a critical deacetylase involved in this process.

Posttranslational modifications of HMGB1 have been described and identified as acetylation,^{6-9,24-26} phosphorylation,^{5,27,28} methylation²⁹ and oxidation.³⁰ Unmodified HMGB1 is the preferred state for its nuclear retention. Posttranslational modifications affect HMGB1 conformation and chromatin binding properties. More specifically, acetylation of lysine residues at positions 2 and 81⁶, and possibly 11, have been shown to affect the ability of HMGB1 to bind to DNA in the nucleus, with similar effects reported for methylation of Lys42.²⁹ Reduced DNA binding predisposes HMGB1 for translocation by either active or passive processes.²⁹ However, the exact mechanisms that are triggered and are responsible for HMGB1 redistribution after its posttranslational modification are unclear but appear to involve CRM1 nuclear exporter, secretory lysosomes,⁷ intracellular calcium mobilization, and activation of the MEK/Erk pathway.²⁵ Despite ambiguity, studies have revealed acetylation of HMGB1's two NLS domains located at residues 27-43 and 177-184 triggers HMGB1's cytoplasmic translocation and entry into the cell export pathway, while HMGB1 phosphorylation prevents its re-entry into the nucleus.^{5,7}

It has been reported that HMGB1 is acetylated by histone acetyltransferases including PCAF, CBP and p300,^{7,26} thereby initiating its translocation. However, it appears that deacetylation is the vital regulator of HMGB1 release, particularly during cellular injury, as it has been shown that loss of nuclear HDAC activity, as a consequence of stress-induced down regulation and HDAC translocation, results in significant HMGB1 release.^{8,9} For instance, studies by Evankovich et al in 2010 revealed that deacetylation and subsequent nuclear retention of HMGB1 in hepatocytes is lost during exposure to oxidative stress because of severely reduced nuclear HDAC1 and -4 activity.⁸ More recently, it was reported that loss of HDAC5 activity due to oxidative stress is also responsible for HMGB1 release in neuronal cells.⁹

The finding that another nuclear deacetylase, SIRT1, is also critically involved in HMGB1 deacetylation broadens the scope of export regulators for this DAMP. At present, it is unknown whether HDAC and SIRT1 cooperate or compete for this substrate, however, the fact that a substantial proportion of HMGB1 can be deacetylated *in vitro* by SIRT1 emphasizes the potential importance of this pathway. Inhibition of SIRT1 or its genetic deletion in endothelial cells, both impair HMGB1 deacetylation and facilitate its cytoplasmic and extracellular translocation both *in vivo* and *in vitro*. Effects of SIRT1 deacetylation of HMGB1 are reinforced by the results of proteomic analysis. MS/MS revealed four lysine residues deacetylated by SIRT1. Interestingly, two of these residues at positions 88 and 90 are within the pro-cytokine domain of HMGB1, while Lys177 is in the RAGE binding domain. Acetylation of other HMG isoforms (including HMGI) has been attributed to a change in their pro-inflammatory capabilities,³¹ but the significance of acetylation of these lysine residues within HMGB1 is unknown. Formation of a disulfide bond between Cys23 and Cys45 impacts the biological function of HMGB1 by converting it from a pro-survival molecule to a pro-damage signal.^{32,33} Acetylation of Lys55 may impact the formation of this disulfide bond. As reported here, loss of SIRT1 deacetylase activity is associated with enhanced HMGB1 release during basal and stress conditions. While it is unclear if the acetylation/deacetylation of lysine residues 55, 88 and 90 impacts HMGB1 translocation and release, SIRT1's ability to deacetylate Lys177 would be expected to affect

its nuclear import as this residue is positioned in the NLS-2. Future mutagenesis studies should reveal actual functionality of individual acetylated lysine residues.

Resveratrol has been shown to directly induce SIRT1 expression at transcriptional and translational levels, while knockdown of SIRT1 has been consistently demonstrated to attenuate many of the effects of resveratrol (reviewed by Hu et al).³⁴ However, reports have described mixed results (dependent on cell type) regarding the ability of resveratrol to influence SIRT1 deacetylase activity.³⁴ It appears that resveratrol can stimulate SIRT1 activity if targeted acetylated lysines are surrounded by hydrophobic residues that allow SIRT1 interaction with the acetylated lysine. A report by Howitz et al²⁰ indicated SIRT1 deacetylation activity is enhanced (due to lowering of the Michaelis constant (K_m)) when targeted acetylated residues are found adjacent to hydrophobic amino acids, especially when bulky hydrophobic aromatic residues, such as tryptophan, tyrosine or phenylalanine are in the +1 and/or +6 position in relation to the acetylated lysine. We observed that HMGB1 lysine residues deacetylated by SIRT1 are located next to hydrophobic residues. Lys55 is adjacent to multiple hydrophobic residues including tryptophan at position +6. Lys88 and Lys90 are also adjacent to multiple hydrophobic residues including phenylalanine at position +1. Although Lys177 is not located next to tryptophan, tyrosine or phenylalanine, it is located within a dense pocket of several hydrophobic residues that flank it on both N- and C-terminal sides. Overall, the 3-D structure of HMGB1 predicts that these lysine residues are exposed on the surface of the molecule and are available for SIRT1 deacetylation.

Notably, SIRT1 itself is the subject of significant regulation under stress conditions or in aged animals. Our group has previously demonstrated that diverse cardiovascular stressors, such as advanced glycation end-products, asymmetric dimethylarginine, or pro-oxidant hydrogen peroxide, each deplete SIRT1 in endothelial cells.²¹ Moreover, we have recently observed that SIRT1's ability to retain HMGB1 in the nucleus is adversely affected as this deacetylase undergoes cytoplasmic translocation during cellular oxidative stress (unpublished data). In addition to this, aging mice show decreased expression of SIRT1 in various tissues.^{20,35} This fact could potentially explain the aging-associated or chronic disease-associated pro-inflammatory profile as a result of SIRT1 deficiency that in turn promotes cellular export of HMGB1.

From the therapeutic standpoint, silencing HMGB1, although technically achievable, could be hazardous as it may devoid the host cells of various housekeeping nuclear functions of this molecule. In contrast, attempts to correct HMGB1 intracellular distribution via SIRT1 activation and improved nuclear retention during stress appear to be more rational. Indeed, there is data demonstrating that the severity of renal injury is reduced in resveratrol-treated animals.³⁶⁻⁴⁴ Our data obtained with resveratrol has a potential to explain this effect mechanistically, as we demonstrate improved HMGB1 nuclear retention in treated mice. Resveratrol pretreatment also showed a tendency to blunt tubular necrosis and leukocyte infiltration 24 hours after bilateral renal IRI. The observation that both the ischemic and unilateral control kidneys of SIRT1 endothelial *-/-* mice sustained considerably worse damage (as compared to SIRT1 Flox/Flox mice) 5 days after unilateral renal IRI further supports the theory that 1) the loss of SIRT1 deacetylase activity enhances the release of

HMGB1 into the circulation during renal injury, and 2) that this circulating DAMP subsequently stimulates renal damage.

If the primary cellular source responsible for release of pro-damage HMGB1 into the circulation during renal injury is the endothelium, then resveratrol treatment would fail to both retain HMGB1 in the nucleus and prevent its release during renal IRI in SIRT1 endothelial $-/-$. While resveratrol pretreatment did cause an increase of nuclear HMGB1 and prevented tubular necrosis in SIRT1 endothelial $-/-$ mice 24 hours after bilateral renal IRI, in contrast, HMGB1 still remained elevated in the circulation. However, resveratrol pretreatment was ineffective in significantly reducing BUN in both genotypes (SIRT1 Flox/Flox and SIRT1 endothelial $-/-$). Collectively, these results indicate multiple cell types are responsible for HMGB1 release during renal injury, such as renal tubular epithelial cells and infiltrating macrophages.

On a broader scale, the finding that HMGB1 is a substrate for SIRT1 deacetylation and is partially responsible for its nuclear retention, adds another dimension to the previously described anti-inflammatory actions of this deacetylase. Inflammation is known to reduce SIRT1 transcription via p53 and hypermethylation in Cancer 1 (HIC1).^{45,46} Furthermore, oxidative stress-induced dissociation of SIRT1-human antigen R (HuR) mRNA complex is known to destabilize SIRT1 mRNA, thus reducing its abundance.⁴⁷ In conclusion, our data alludes to a vicious cycle in which the inflammation-induced repression of SIRT1 disables deacetylation of HMGB1 and facilitates its nuclear-to-cytoplasmic translocation and systemic release, thus maintaining inflammation.

Materials and Methods

Animal Models

Mice used in experiments were FVB/NJ (Jackson Laboratories) and B6:129 with endothelial specific deletion of SIRT1, as described in the Supplementary Methods online.

Renal Ischemia-Reperfusion Injury Model

Surgeries on both mice strains (FVB/NJ mice and B6:129 mice with endothelial SIRT1 deletion) were conducted as previously described,¹³ (Supplementary Methods online). Details of resveratrol pretreatment are also described in the Supplementary Methods online.

Endothelial Cell Cultures

Primary cultures of endothelial cells were established from sprouting aortic rings taken from SIRT1 endothelial $-/-$, as previously described.^{48,49} The endothelial cell line Ea.hy926 (ATCC, Manassas, VA) was also used in experiments. Details of cell culturing and treatment with SIRT1 inhibitor are described in the Supplementary Methods online.

Isolation of Cytoplasmic and Nuclear Proteins

To obtain cytoplasmic and nuclear fractions from whole kidney tissue or cultured cells, subcellular and nuclear fractionation protocols were utilized,^{13,25} (Supplementary Methods online).

Analysis of Acetylated HMGB1 by Immunoprecipitation

Immunoprecipitation of acetylated HMGB1 from nuclear and cytoplasmic fractions using HMGB1 antibody (Abcam, Cambridge, MA), followed by Western blot analysis using acetylated lysine antibodies (Abcam), was conducted according to manufacturer's protocol (Santa Cruz Biotech),²⁵ (Supplementary Methods online).

HMGB1-GFP Plasmid Transfection

Immortalized HUVEC were transfected with HMGB1-GFP plasmid using the Amaxa HUVEC Nucleofector Kit (Lonza) and Amaxa Biosystems Nucleofector II Transfection Unit (Lonza), as previously described.¹³ Treatment of cells with LPS and/or SIRT1 inhibitor and subsequent analysis is described in the Supplementary Methods online.

SIRT1 Deacetylation of HMGB1

After immunoprecipitation, acetylated HMGB1 was used for analysis of SIRT1 mediated deacetylation of HMGB1 in an *in vitro* assay, (Supplementary Methods online).

Identification of SIRT1 Deacetylation Sites on HMGB1

Acetylated HMGB1 was obtained from whole kidney homogenates of control and SIRT1 endothelial +/- kidneys (subjected to 30 minutes of renal IRI) and incubated with rSIRT1 for analysis of SIRT1 mediated deacetylation. (See Supplementary Methods online for full details about HMGB1 deacetylation, isolation and Applied Biomics mass spectrometry analysis).

The 3-D protein structures were acquired from RCSB Protein Databank and visualized with the PyMOL Molecular Graphics Systems software, Version 1.5.0.4 Schrödinger, LLC (Supplementary Methods online).

Western Blot Analysis

HMGB1 and acetylated HMGB1 were examined in samples by Western blotting, as previously described,²⁵ (Supplementary Methods online).

Immunocytochemistry Staining for HMGB1

Immunocytochemistry was performed on immortalized HUVEC treated with LPS and/or SIRT1 inhibitor (Supplementary Methods online). HMGB1 localization in the nucleus and cytoplasm was quantified using NIH's ImageJ (Supplementary Methods online).

Histology

Kidneys were fixed with 4% paraformaldehyde, paraffin embedded, sectioned and stained. Details of staining and histological analysis of renal injury are described in the Supplementary Methods online.

Renal Function Analysis

Plasma was obtained by cardiac puncture and samples were analyzed for creatinine concentration (Thermo Scientific's creatinine assay kit) and BUN (Arbor Assay's BUN kit; Ann Arbor, Michigan).

HMGB1 Elisa Kit

Nuclear and cytoplasmic fractions, urine and plasma were all analysed for HMGB1 content using a HMGB1 ELISA Kit and protocol (Neobiolab, Cambridge, MA).

Statistical analysis

Details of statistical analysis are reported in the Supplementary Methods online.

Supplementary Material

Refer to Web version on PubMed Central for supplementary material.

Acknowledgments

Studies were supported by NIH grants DK54602, DK052783 and DK45462 (MSG), AHA grant 12SDG9080006 (BBR), and the Westchester Artificial Kidney Foundation. Authors are indebted to Dr. Samuel H. Wilson (Laboratory of Structural Biology, NIEHS, NIH) for sharing the HMGB1-GFP construct used in these studies.

References

1. Tang D, Kang R, Livesey KM, et al. High-mobility group box 1 is essential for mitochondrial quality control. *Cell Metab.* 2011; 13:701–711. [PubMed: 21641551]
2. Scaffidi P, Misteli T, Bianchi ME. Release of chromatin protein HMGB1 by necrotic cells triggers inflammation. *Nature.* 2002; 418:191–195. [PubMed: 12110890]
3. Gardella S, Andrei C, Ferrera D, et al. The nuclear protein HMGB1 is secreted by monocytes via a non-classical, vesicle-mediated secretory pathway. *EMBO Rep.* 2002; 3:995–1001. [PubMed: 12231511]
4. Tang D, Kang R, Zeh HJ 3rd, et al. High-mobility group box 1, oxidative stress, and disease. *Antioxid Redox Signal.* 2011; 14:1315–1335. [PubMed: 20969478]
5. Youn JH, Shin JS. Nucleocytoplasmic shuttling of HMGB1 is regulated by phosphorylation that redirects it toward secretion. *J Immunol.* 2006; 177:7889–7897. [PubMed: 17114460]
6. Elenkov I, Pelovsky P, Ugrinova I, et al. The DNA binding and bending activities of truncated tail-less HMGB1 protein are differentially affected by Lys-2 and Lys-81 residues and their acetylation. *Int J Biol Sci.* 2011; 7:691–699. [PubMed: 21647302]
7. Bonaldi T, Talamo F, Scaffidi P, et al. Monocytic cells hyperacetylate chromatin protein HMGB1 to redirect it towards secretion. *EMBO J.* 2003; 22:5551–5560. [PubMed: 14532127]
8. Evankovich J, Cho SW, Zhang R, et al. High mobility group box 1 release from hepatocytes during ischemia and reperfusion injury is mediated by decreased histone deacetylase activity. *J Biol Chem.* 2010; 285:39888–39897. [PubMed: 20937823]
9. He M, Zhang B, Wei X, et al. HDAC4/5-HMGB1 signalling mediated by NADPH oxidase activity contributes to cerebral ischaemia/reperfusion injury. *J Cell Mol Med.* 2013; 17:531–542. [PubMed: 23480850]
10. Tanno M, Sakamoto J, Miura T, et al. Nucleocytoplasmic shuttling of the NAD⁺-dependent histone deacetylase SIRT1. *J Biol Chem.* 2007; 282:6823–6832. [PubMed: 17197703]
11. Andrassy M, Volz HC, Igwe JC, et al. High-mobility group box-1 in ischemia-reperfusion injury of the heart. *Circulation.* 2008; 117:3216–3226. [PubMed: 18574060]

12. Yang QW, Lu FL, Zhou Y, et al. HMGB1 mediates ischemia-reperfusion injury by TRIF-adaptor independent Toll-like receptor 4 signaling. *J Cereb Blood Flow Metab.* 2011; 31:593–605. [PubMed: 20700129]
13. Rabadi MM, Ghaly T, Goligorsky MS, et al. HMGB1 in renal ischemic injury. *Am J Physiol Renal Physiol.* 2012; 303:F873–885. [PubMed: 22759395]
14. Wu H, Ma J, Wang P, et al. HMGB1 contributes to kidney ischemia reperfusion injury. *J Am Soc Nephrol.* 2010; 21:1878–1890. [PubMed: 20847143]
15. Ratliff BB, Rabadi MM, Vasko R, et al. Messengers without borders: mediators of systemic inflammatory response in AKI. *J Am Soc Nephrol.* 2013; 24:529–536. [PubMed: 23349311]
16. Mullins GE, Sunden-Cullberg J, Johansson AS, et al. Activation of human umbilical vein endothelial cells leads to relocation and release of high-mobility group box chromosomal protein 1. *Scand J Immunol.* 2004; 60:566–573. [PubMed: 15584967]
17. Ulloa L, Ochani M, Yang H, et al. Ethyl pyruvate prevents lethality in mice with established lethal sepsis and systemic inflammation. *Proc Natl Acad Sci U S A.* 2002; 99:12351–12356. [PubMed: 12209006]
18. Lang CH, Silvis C, Deshpande N, et al. Endotoxin stimulates in vivo expression of inflammatory cytokines tumor necrosis factor alpha, interleukin-1beta, -6, and high-mobility-group protein-1 in skeletal muscle. *Shock.* 2003; 19:538–546. [PubMed: 12785009]
19. Tian XX, Wu CX, Sun H, et al. [Ethyl pyruvate inhibited HMGB1 expression induced by LPS in macrophages]. *Xi Bao Yu Fen Zi Mian Yi Xue Za Zhi.* 2011; 27:1304–1307. 1311. [PubMed: 22152811]
20. Howitz KT, Bitterman KJ, Cohen HY, et al. Small molecule activators of sirtuins extend *Saccharomyces cerevisiae* lifespan. *Nature.* 2003; 425:191–196. [PubMed: 12939617]
21. Chen J, Xavier S, Moskowitz-Kassai E, et al. Cathepsin cleavage of sirtuin 1 in endothelial progenitor cells mediates stress-induced premature senescence. *Am J Pathol.* 2012; 180:973–983. [PubMed: 22234173]
22. Haigis MC, Sinclair DA. Mammalian sirtuins: biological insights and disease relevance. *Annu Rev Pathol.* 2010; 5:253–295. [PubMed: 20078221]
23. Westphal CH, Dipp MA, Guarente L. A therapeutic role for sirtuins in diseases of aging? *Trends Biochem Sci.* 2007; 32:555–560. [PubMed: 17980602]
24. Dhupar R, Klune JR, Evankovich J, et al. Interferon regulatory factor 1 mediates acetylation and release of high mobility group box 1 from hepatocytes during murine liver ischemia-reperfusion injury. *Shock.* 2011; 35:293–301. [PubMed: 20856174]
25. Rabadi MM, Kuo MC, Ghaly T, et al. Interaction between uric acid and HMGB1 translocation and release from endothelial cells. *Am J Physiol Renal Physiol.* 2012; 302:F730–741. [PubMed: 22189943]
26. Ong SP, Lee LM, Leong YF, et al. Dengue virus infection mediates HMGB1 release from monocytes involving PCAF acetylase complex and induces vascular leakage in endothelial cells. *PLoS One.* 2012; 7:e41932. [PubMed: 22860034]
27. Lee H, Park M, Shin N, et al. High mobility group box-1 is phosphorylated by protein kinase C zeta and secreted in colon cancer cells. *Biochem Biophys Res Commun.* 2012; 424:321–326. [PubMed: 22750245]
28. Oh YJ, Youn JH, Ji Y, et al. HMGB1 is phosphorylated by classical protein kinase C and is secreted by a calcium-dependent mechanism. *J Immunol.* 2009; 182:5800–5809. [PubMed: 19380828]
29. Ito I, Fukazawa J, Yoshida M. Post-translational methylation of high mobility group box 1 (HMGB1) causes its cytoplasmic localization in neutrophils. *J Biol Chem.* 2007; 282:16336–16344. [PubMed: 17403684]
30. Hoppe G, Talcott KE, Bhattacharya SK, et al. Molecular basis for the redox control of nuclear transport of the structural chromatin protein Hmgb1. *Exp Cell Res.* 2006; 312:3526–3538. [PubMed: 16962095]
31. Banks GC, Li Y, Reeves R. Differential in vivo modifications of the HMGI(Y) nonhistone chromatin proteins modulate nucleosome and DNA interactions. *Biochemistry.* 2000; 39:8333–8346. [PubMed: 10889043]

32. Venereau E, Casagrandi M, Schiraldi M, et al. Mutually exclusive redox forms of HMGB1 promote cell recruitment or proinflammatory cytokine release. *J Exp Med.* 2012; 209:1519–1528. [PubMed: 22869893]
33. Yang H, Lundback P, Ottosson L, et al. Redox modification of cysteine residues regulates the cytokine activity of high mobility group box-1 (HMGB1). *Mol Med.* 2012; 18:250–259. [PubMed: 22105604]
34. Hu Y, Liu J, Wang J, et al. The controversial links among calorie restriction, SIRT1, and resveratrol. *Free Radic Biol Med.* 2011; 51:250–256. [PubMed: 21569839]
35. Guarente L, Franklin H. Epstein Lecture: Sirtuins, aging, and medicine. *N Engl J Med.* 2011; 364:2235–2244. [PubMed: 21651395]
36. Chander V, Turkey N, Chopra K. Resveratrol, a polyphenolic phytoalexin protects against cyclosporine-induced nephrotoxicity through nitric oxide dependent mechanism. *Toxicology.* 2005; 210:55–64. [PubMed: 15804458]
37. Sener G, Tugtepe H, Yuksel M, et al. Resveratrol improves ischemia/reperfusion-induced oxidative renal injury in rats. *Arch Med Res.* 2006; 37:822–829. [PubMed: 16971220]
38. Kitada M, Kume S, Imaizumi N, et al. Resveratrol improves oxidative stress and protects against diabetic nephropathy through normalization of Mn-SOD dysfunction in AMPK/SIRT1-independent pathway. *Diabetes.* 2011; 60:634–643. [PubMed: 21270273]
39. Palsamy P, Subramanian S. Resveratrol protects diabetic kidney by attenuating hyperglycemia-mediated oxidative stress and renal inflammatory cytokines via Nrf2-Keap1 signaling. *Biochim Biophys Acta.* 2011; 1812:719–731. [PubMed: 21439372]
40. Chang CC, Chang CY, Wu YT, et al. Resveratrol retards progression of diabetic nephropathy through modulations of oxidative stress, proinflammatory cytokines, and AMP-activated protein kinase. *J Biomed Sci.* 2011; 18:47. [PubMed: 21699681]
41. Do Amaral CL, Francescato HD, Coimbra TM, et al. Resveratrol attenuates cisplatin-induced nephrotoxicity in rats. *Arch Toxicol.* 2008; 82:363–370. [PubMed: 18026934]
42. Chander V, Chopra K. Protective effect of resveratrol, a polyphenolic phytoalexin on glycerol-induced acute renal failure in rat kidney. *Ren Fail.* 2006; 28:161–169. [PubMed: 16538975]
43. Holthoff JH, Wang Z, Seely KA, et al. Resveratrol improves renal microcirculation, protects the tubular epithelium, and prolongs survival in a mouse model of sepsis-induced acute kidney injury. *Kidney Int.* 2012; 81:370–378. [PubMed: 21975863]
44. He W, Wang Y, Zhang MZ, et al. Sirt1 activation protects the mouse renal medulla from oxidative injury. *J Clin Invest.* 2010; 120:1056–1068. [PubMed: 20335659]
45. Li P, Zhao Y, Wu X, et al. Interferon gamma (IFN-gamma) disrupts energy expenditure and metabolic homeostasis by suppressing SIRT1 transcription. *Nucleic Acids Res.* 2012; 40:1609–1620. [PubMed: 22064865]
46. Zhang Q, Wang SY, Fleuriel C, et al. Metabolic regulation of SIRT1 transcription via a HIC1:CtBP corepressor complex. *Proc Natl Acad Sci U S A.* 2007; 104:829–833. [PubMed: 17213307]
47. Abdelmohsen K, Pullmann R Jr, Lal A, et al. Phosphorylation of HuR by Chk2 regulates SIRT1 expression. *Mol Cell.* 2007; 25:543–557. [PubMed: 17317627]
48. Brodsky SV, Gealekman O, Chen J, et al. Prevention and reversal of premature endothelial cell senescence and vasculopathy in obesity-induced diabetes by ebselen. *Circ Res.* 2004; 94:377–384. [PubMed: 14670841]
49. Brodsky SV, Zhang F, Nasjletti A, et al. Endothelium-derived microparticles impair endothelial function in vitro. *Am J Physiol Heart Circ Physiol.* 2004; 286:H1910–1915. [PubMed: 15072974]
50. Conger JD, Schultz MF, Miller F, et al. Responses to hemorrhagic arterial pressure reduction in different ischemic renal failure models. *Kidney Int.* 1994; 46:318–323. [PubMed: 7967342]

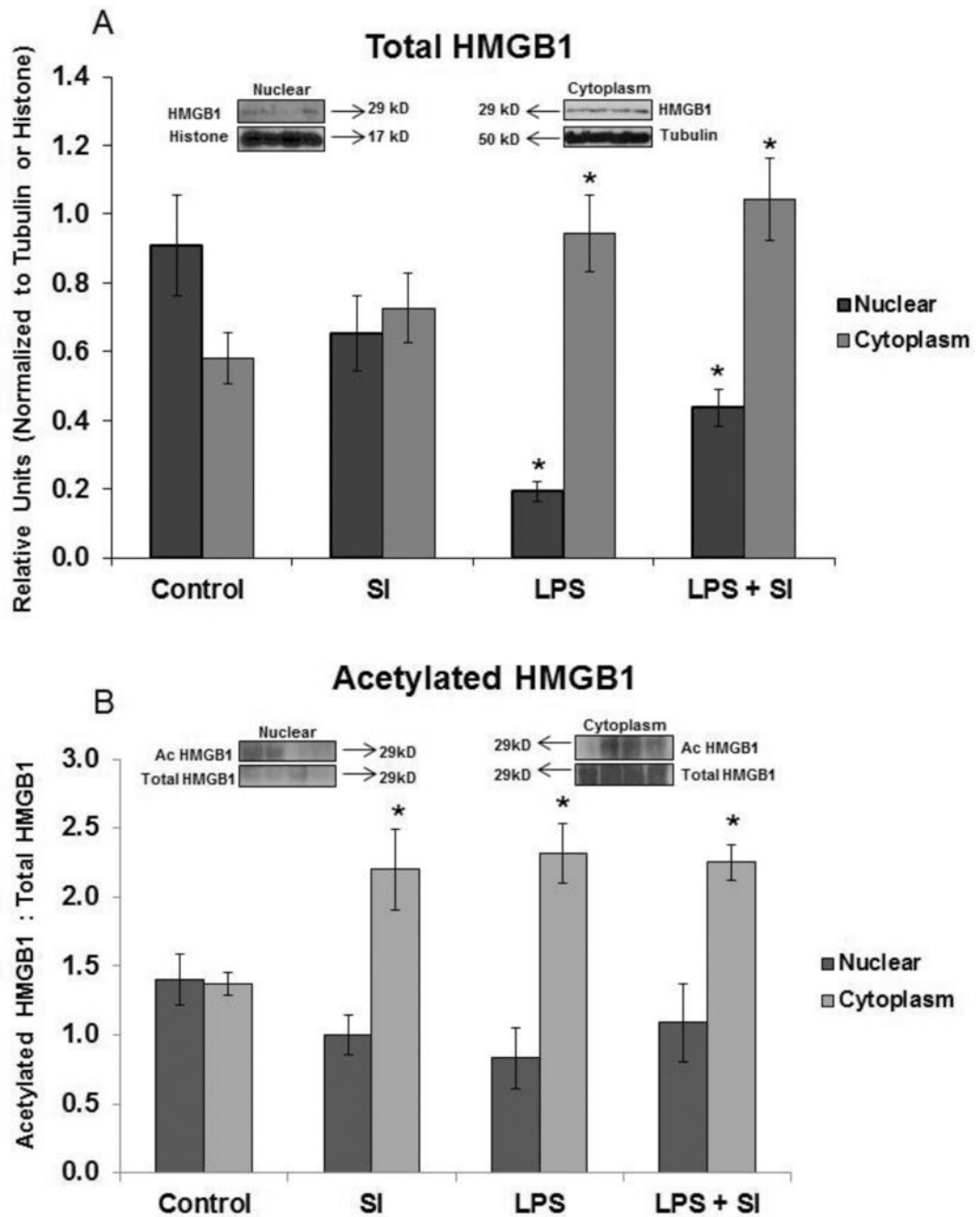


Figure 1. Total and acetylated HMGB1 in HUVEC treated for 4 hours with LPS and SIRT1 inhibitor (SI)

HUVEC treated with SI and LPS for 4 hours demonstrated enhanced translocation (A) and acetylation (B) under basal conditions and when treated with LPS. However, translocated and acetylated HMGB1 did not differ between SI and LPS + SI treatments, indicating lack of additive effect. *p 0.05 vs. control; n=6 panel A; n=3-5 panel B.

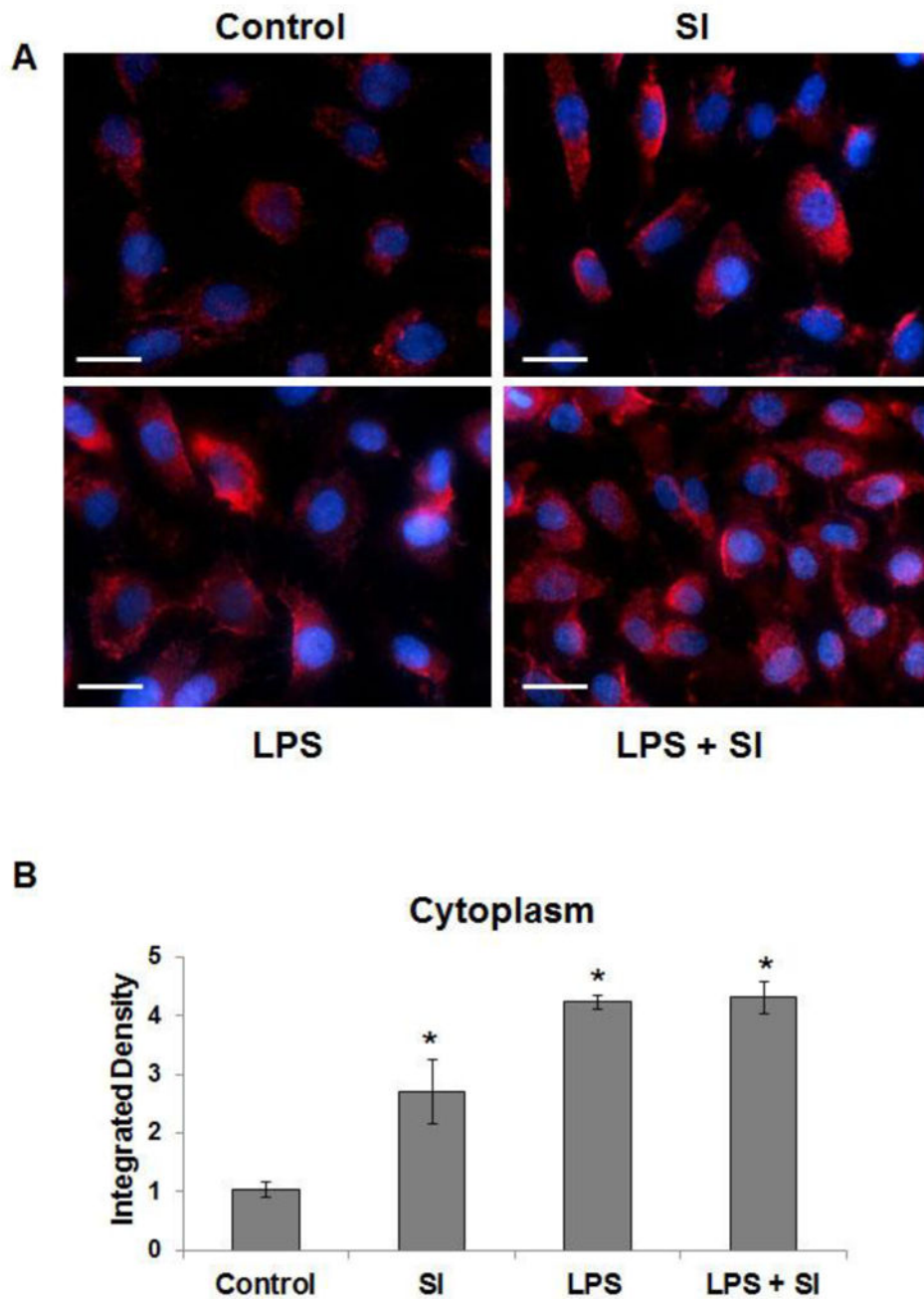


Figure 2. HUVEC stained for HMGB1 after 24 hours of LPS and SIRT1 inhibitor (SI) treatment (A) HMGB1 immunocytochemistry and (B) quantification of fluorescence intensity demonstrated that HUVEC treated with SIRT1 inhibitor (SI) and LPS for 24 hours showed enhanced translocation from the nucleus to the cytoplasm, as compared to control cells. HMGB1 did not differ between SI and LPS + SI treatment, suggesting the lack of additive effect. * $p < 0.05$ vs. control; $n = 3$. All images are 600x magnification. Scale bar represents 25 μm .

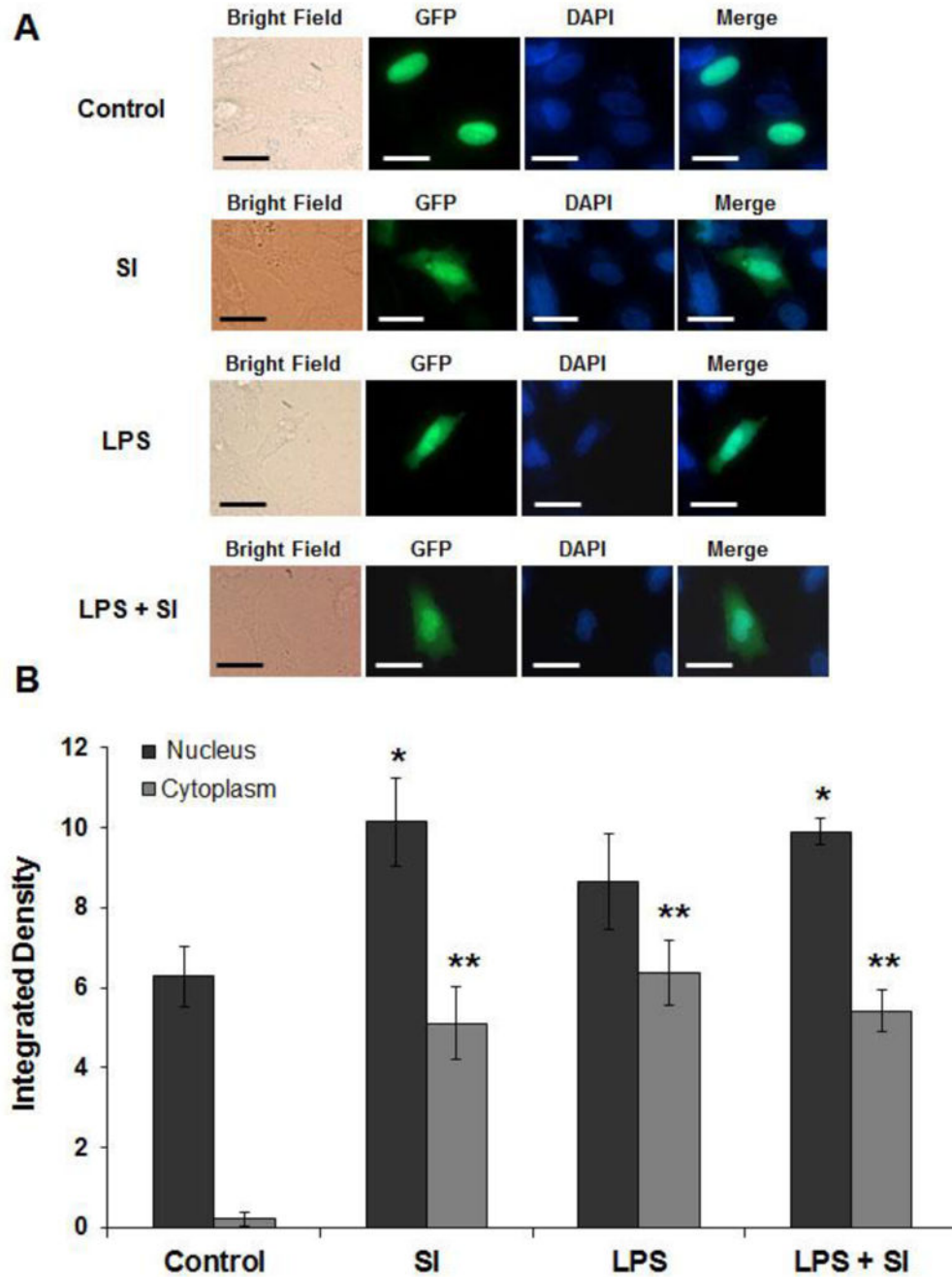


Figure 3. HUVEC transfected with HMGB1-GFP plasmid treated for 24 hours with SIRT1 inhibitor (SI) with and without LPS

(A) Fixed transfected cells imaged for HMGB1-GFP translocation and (B) quantification of fluorescence intensity demonstrated that SIRT1 inhibitor increased HMGB1 nuclear-to-cytoplasmic translocation, as indicated by increased GFP fluorescence in the cytoplasm. Administration of LPS also promoted HMGB1 translocation to the cytoplasm. LPS and SIRT1 inhibitor co-administration did not further enhance HMGB1 cytosolic fluorescence, suggesting that both activate similar mechanisms. At longer times, LPS and SIRT1 inhibitor treatment increased HMGB1-GFP fluorescence in the nucleus, suggesting increased protein

expression. * $p < 0.05$ vs. nuclear control; ** $p < 0.05$ vs. cytoplasmic control; $n = 5$. All images are 600x magnification. Scale bar represents 25 μm .

Author Manuscript

Author Manuscript

Author Manuscript

Author Manuscript

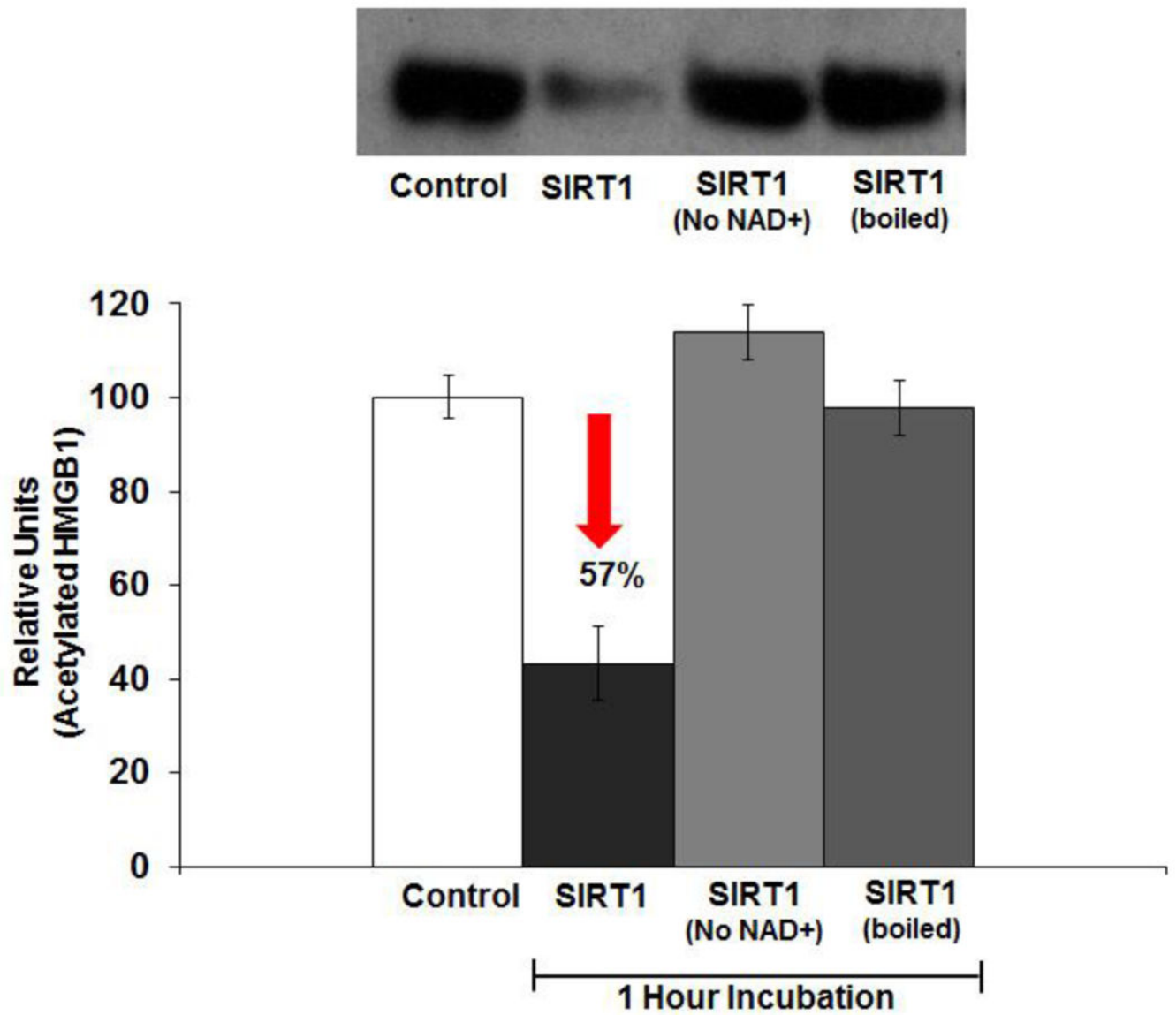


Figure 4. SIRT1 deacetylation of HMGB1

Immunoprecipitated acetylated (Ac) HMGB1 was combined with recombinant SIRT1 for 60 minutes and levels of acetylated HMGB1 were quantified by immunoblotting. SIRT1 deacetylated HMGB1 by 49% within 1 hour. * $p > 0.05$ vs. untreated; $n = 7$.

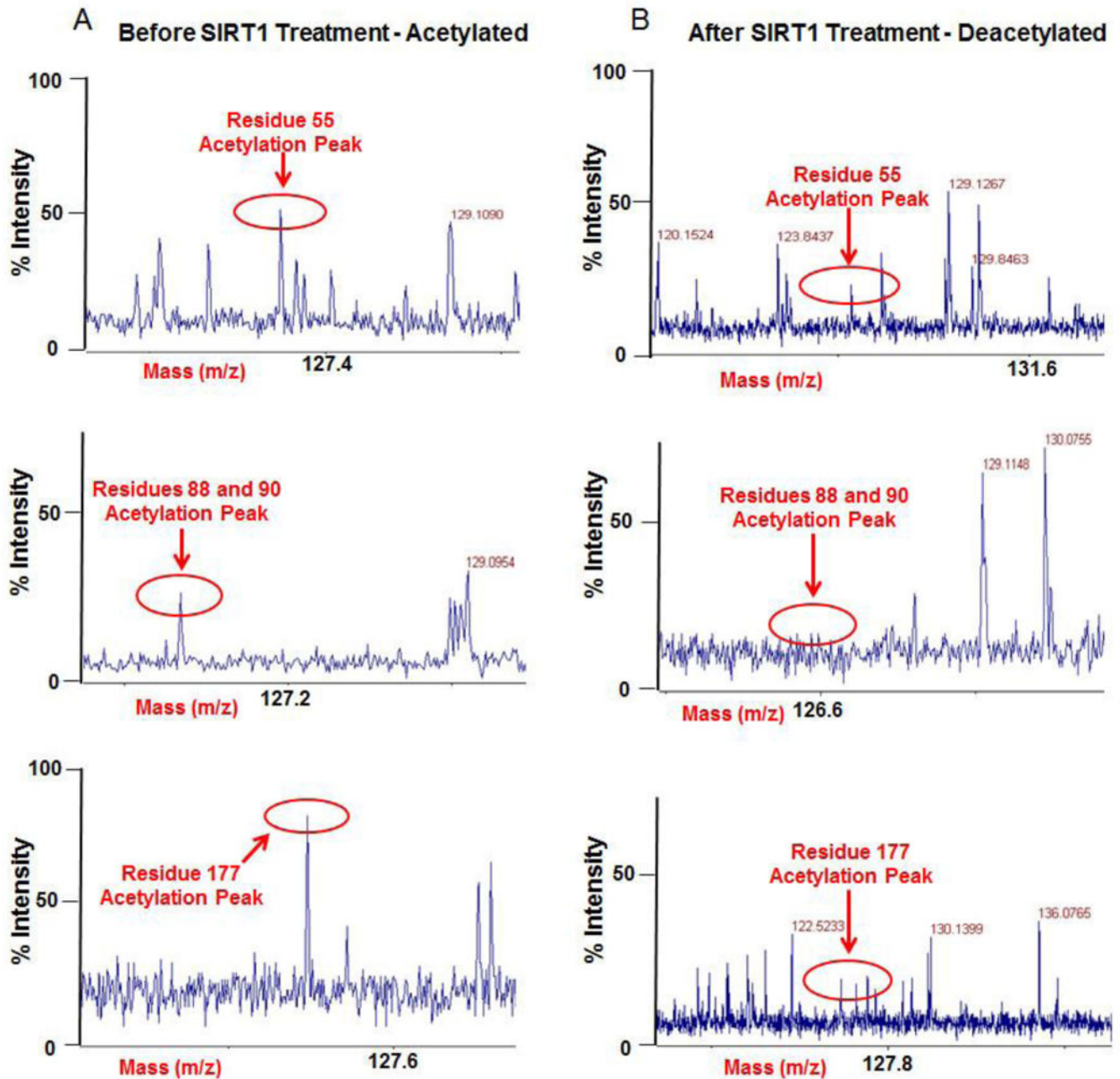


Figure 5. Mass spectrometry analysis of the lysine residues in HMGB1 that are deacetylated by SIRT1

Purified acetylated HMGB1 was incubated with SIRT1 and cofactors at 37°C for 1 hour. Subsequently, HMGB1 was examined by mass spectrometry. HMGB1 in samples was proteolytically fragmented with trypsin prior to mass spectrometry analysis, as detailed in Methods. Acetylated lysine residues appeared on the MS/MS spectra as peaks at 126 m/z. Before SIRT1 treatment, lysine residues 55, 88, 90 and 177 were acetylated (A), however, after SIRT1 treatment these residues were no longer acetylated (B), indicating SIRT1 deacetylation.

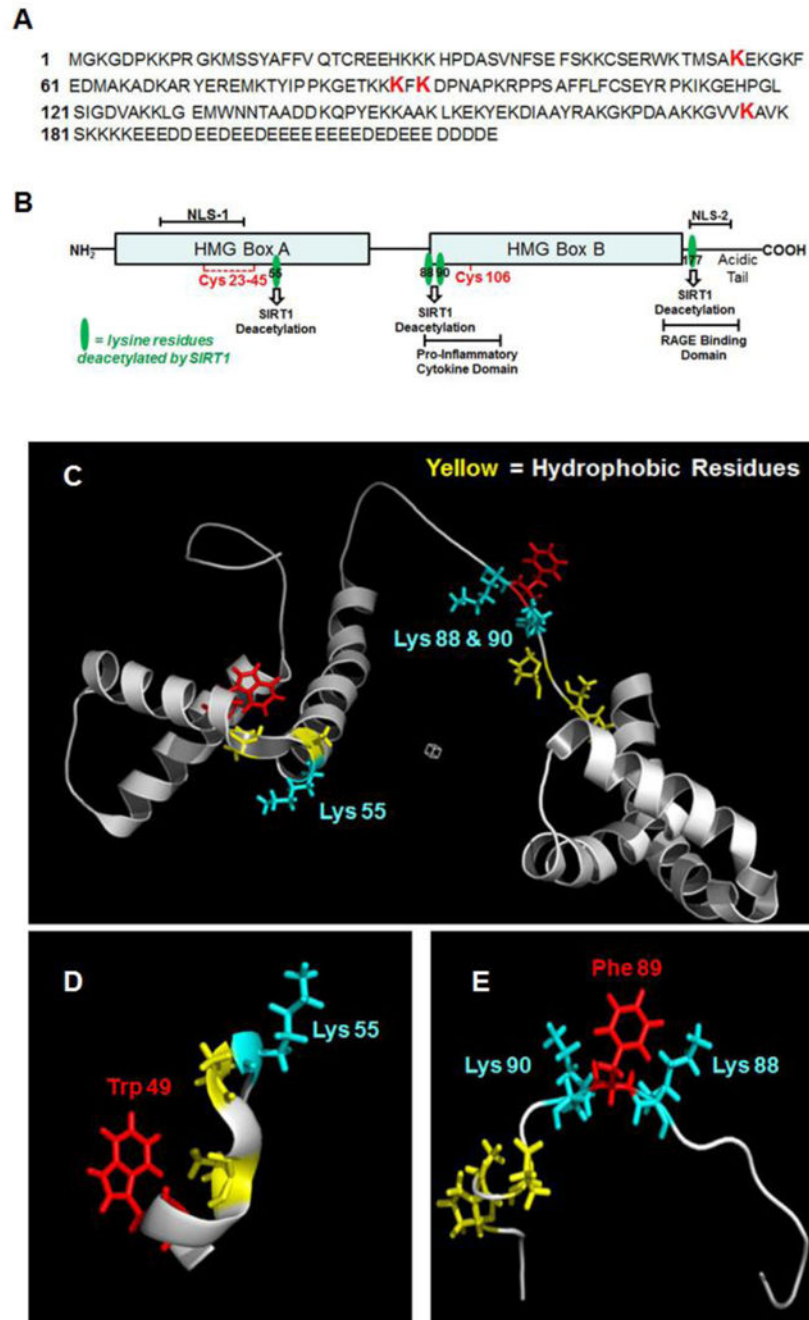


Figure 6. Illustration of the lysine residues deacetylated by SIRT1, as determined by mass spectrometry analysis

(A) Mass spectrometry analysis revealed lysine residues (K) at positions 55, 88, 90 and 177 (highlighted in red text) within the 215 amino acid sequence of HMGB1 are deacetylated by SIRT1. (B) The positions of the deacetylated residues in the HMG Box A and Box B are shown. Lys55 is in HMG Box A adjacent to Cys45. Lysine residues 88 and 90 are in the pro-inflammatory cytokine domain. Lys177 is in the NLS-2 and RAGE-binding domain. (C) The 3-D protein structure of HMGB1 shows the location of SIRT1 deacetylated lysines (highlighted in blue) in relation to hydrophobic residues (highlighted in yellow), including

the presence of large bulky aromatic tryptophan and phenylalanine residues (highlighted in red) adjacent to Lys55 (D) and Lys88 and Lys90 (E), respectively. The 3-D protein structure for the entire HMGB1 for positioning of Lys177 is currently not available. References for the HMGB1 3-D protein structure are in the Methods section.

Author Manuscript

Author Manuscript

Author Manuscript

Author Manuscript

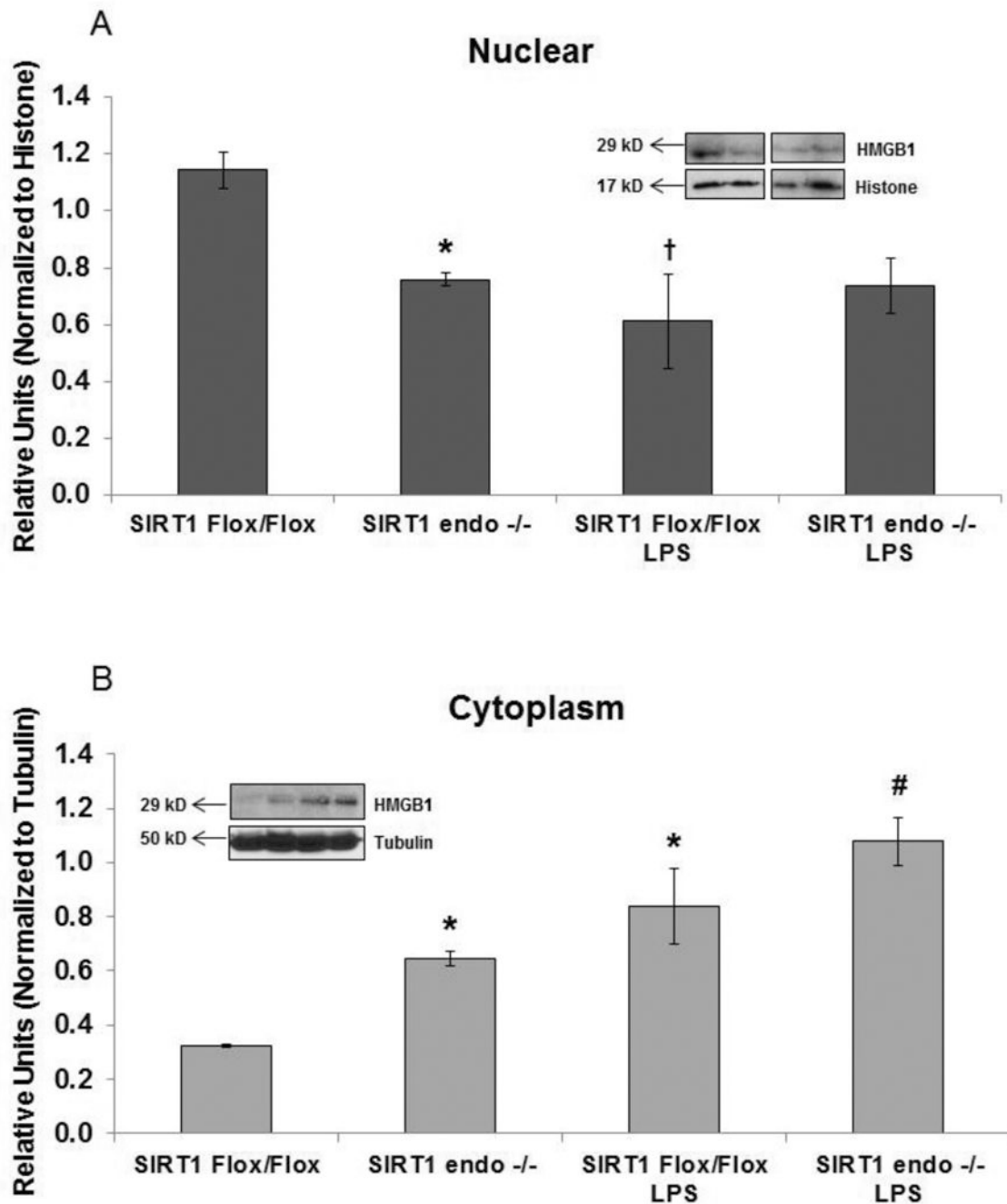


Figure 7. Nuclear (A) and cytoplasmic (B) HMGB1 in SIRT1 Flox/Flox and SIRT1 endothelial -/- cell primary cultures from the aorta treated with LPS for 4 hours

SIRT1 endothelial -/- cells demonstrated enhanced cytoplasmic translocation under basal conditions and LPS treatment. Nuclear Western blot images for HMGB1 were obtained from different parts of the same gel. * $p < 0.05$ vs. SIRT1 Flox/Flox; # $p < 0.05$ vs. SIRT1 endothelial -/-; † $p < 0.10$ vs. SIRT1 Flox/Flox; $n = 4$.

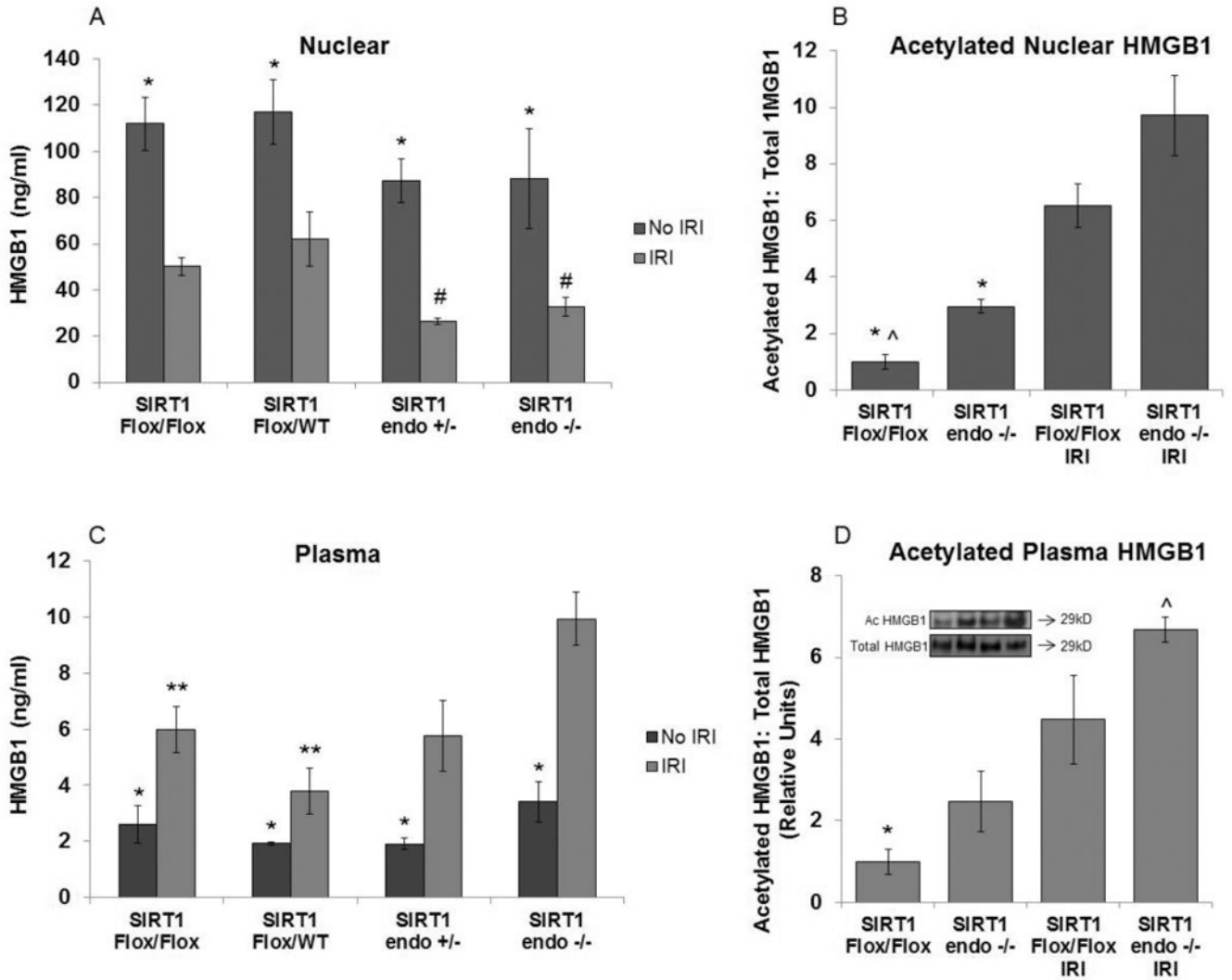


Figure 8. Nuclear and plasma HMGB1 in endothelial SIRT1 endothelial -/- mice after renal IRI Mice were subjected to 30 minutes of bilateral renal IRI and examined for HMGB1 translocation 1 hour after reperfusion. As measured by ELISA and immunoblotting, the SIRT1 endothelial -/- cells resulted in reduced nuclear HMGB1 (A) and increased proportion of nuclear acetylated HMGB1 (B), as compared to SIRT1 Flox/Flox mice. Total HMGB1 (C) and acetylated HMGB1 (D) increased in the circulation after renal IRI in SIRT1 Flox/Flox, heterozygous SIRT1 endothelial +/- and SIRT1 endothelial -/- mice with the most robust increase occurring in endothelial SIRT1 endothelial -/- mice. Data in figures lacking Western blot images were obtained by ELISA assay. In Fig 9B, acetylated HMGB1 was quantified by Western blot, while total HMGB1 was quantified by ELISA. *p<0.05 vs. IRI groups; #p<0.05 vs. SIRT1 Flox/Flox IRI; ^p<0.01 vs. SIRT1 endothelial -/-; **P<0.05 vs. SIRT1 endothelial -/- IRI; n=4-5.

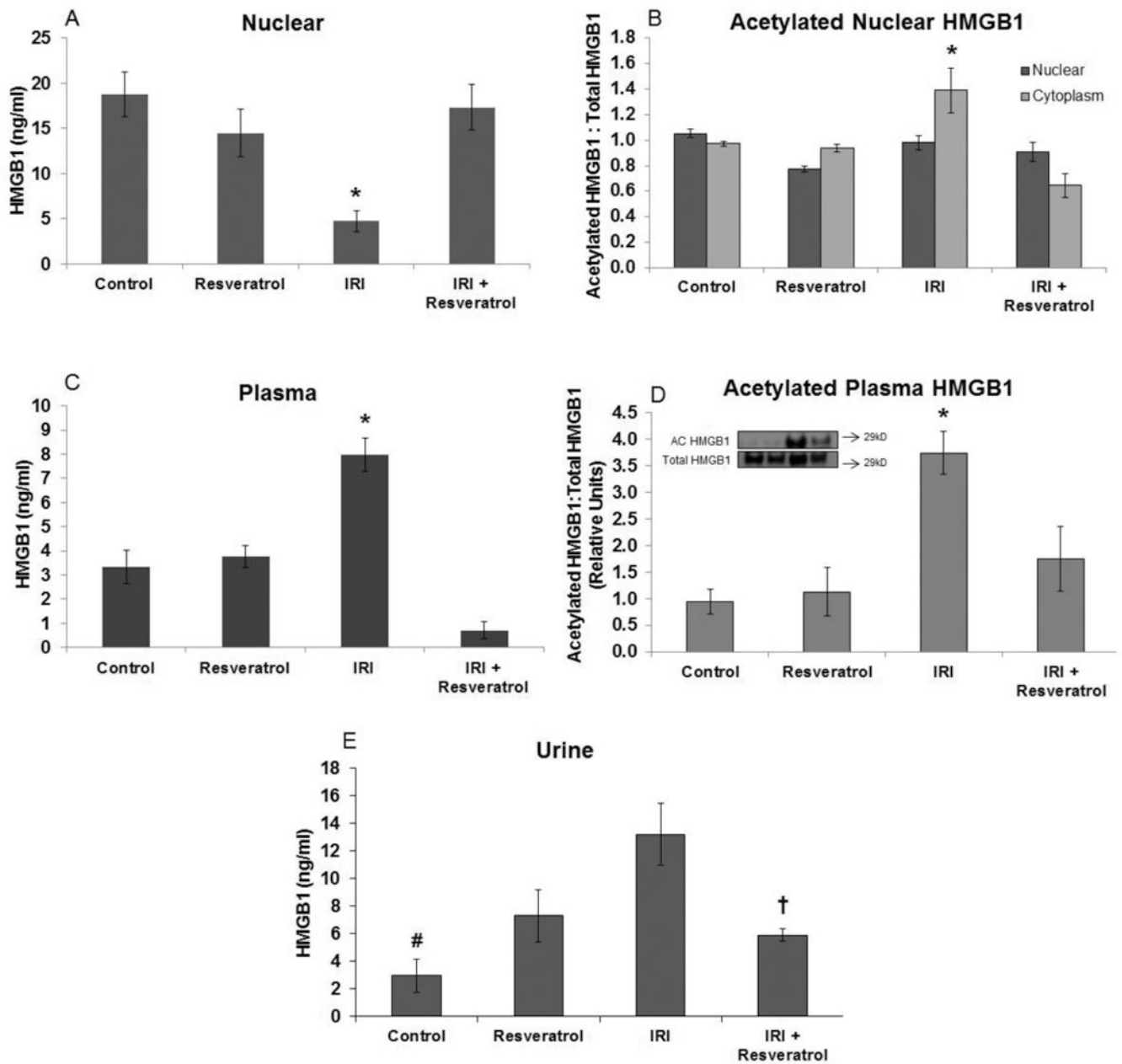


Figure 9. FVB/NJ mice pre-treated with SIRT1 activator resveratrol prior to renal IRI
 Pretreatment with resveratrol prior to bilateral renal IRI resulted in improved HMGB1 nuclear (A) retention 1 hour after IRI. IRI enhanced levels of acetylated HMGB1 in the cytoplasm (B) 1 hour after IRI, but pretreatment with resveratrol normalized HMGB1 acetylation. Total HMGB1 (C) and acetylated HMGB1 (D) increased in the circulation 1 hour after IRI, but were significantly decreased by resveratrol. HMGB1 was elevated in the urine (E) 24 hours after IRI, but was reduced by resveratrol pretreatment. Data in figures lacking Western blot images were obtained by ELISA assay. In Fig 9B, acetylated HMGB1 was quantified by Western blot while total HMGB1 was quantified by ELISA. *p 0.05 vs. all groups; #p<0.05 vs. IRI; †p<0.10 vs. IRI; n=3-5.

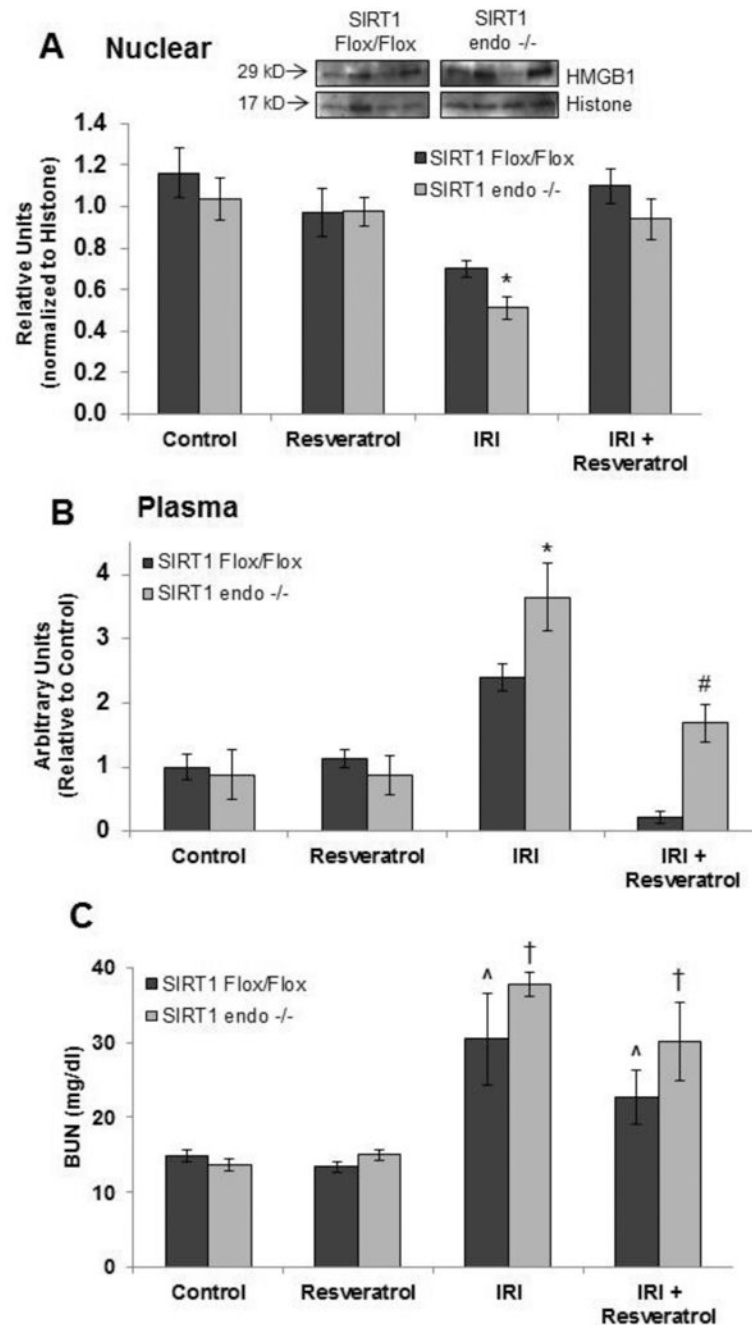


Figure 10. Comparison of the effects of resveratrol pretreatment in SIRT1 Flox/Flox versus SIRT1 endothelial -/- mice

Similar to the affect observed in FVB/NJ, 1 hour after a 30 minute episode of bilateral renal IRI, nuclear levels of HMGB1 were reduced (A) while circulating HMGB1 was enhanced (B) in SIRT1 Flox/Flox mice, an effect that was potentiated when SIRT1 was ablated in endothelial cells. While resveratrol pretreatment prevented the reduction of nuclear HMGB1 during IRI, circulating levels of HMGB1 remained elevated. Bilateral IRI resulted in a rise in BUN in both SIRT1 Flox/Flox and SIRT1 endothelial -/- mice 24 hours after IRI (C). There was a numerical (but statistically insignificant) difference in BUN levels between

SIRT1 Flox/Flox and SIRT1 endothelial -/mice after bilateral IRI and resveratrol pretreatment. *p < 0.05 vs. SIRT1 Flox/Flox IRI; ^p < 0.05 vs. SIRT1 Flox/Flox control; †p < 0.05 vs. SIRT1 endothelial -/- control; #p < 0.10 vs. SIRT1 Flox/Flox IRI + resveratrol; n=3-5.

Author Manuscript

Author Manuscript

Author Manuscript

Author Manuscript

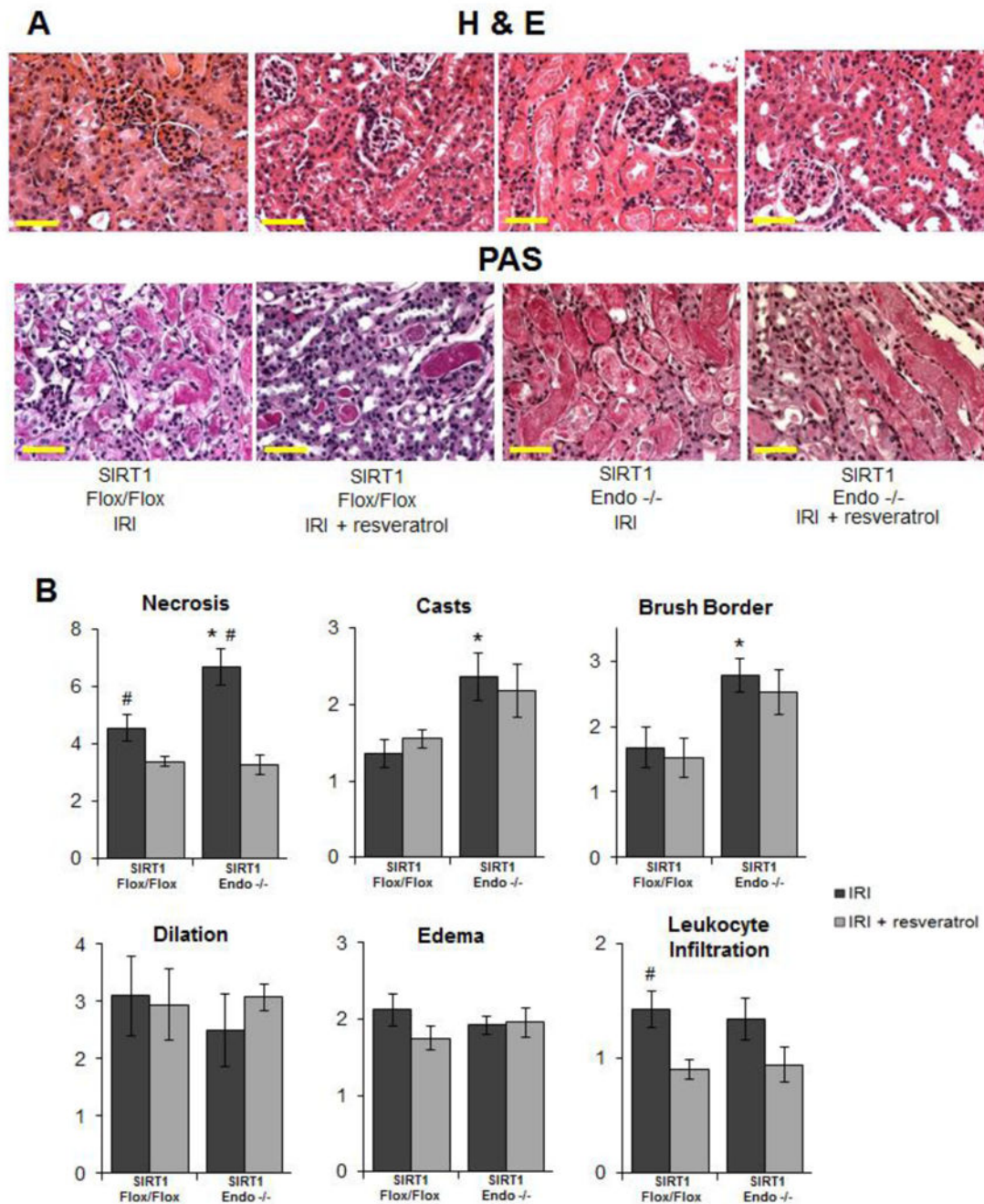


Figure 11. Histological analysis of renal damage in SIRT1 Flox/Flox and SIRT1 endothelial -/- mice 24 hours after a 30 minute episode of bilateral renal IRI

SIRT1 endothelial -/- mice exhibited worse renal damage after IRI, including enhanced tubular epithelial cell necrosis, loss of brush border and cast formation, as indicated by hemotoxylin and eosin and periodic acid-shift staining (A) and quantified for pathological score (B), as described by Conger et al.⁵⁰ Resveratrol pretreatment attenuated necrosis, but had negligible effects on all other examined parameters. * $p < 0.10$ vs. SIRT1 Flox/Flox IRI; # $p < 0.10$ vs. resveratrol (same group); $n = 3$. All images are 400x magnification. Scale bar represents 50 μm .

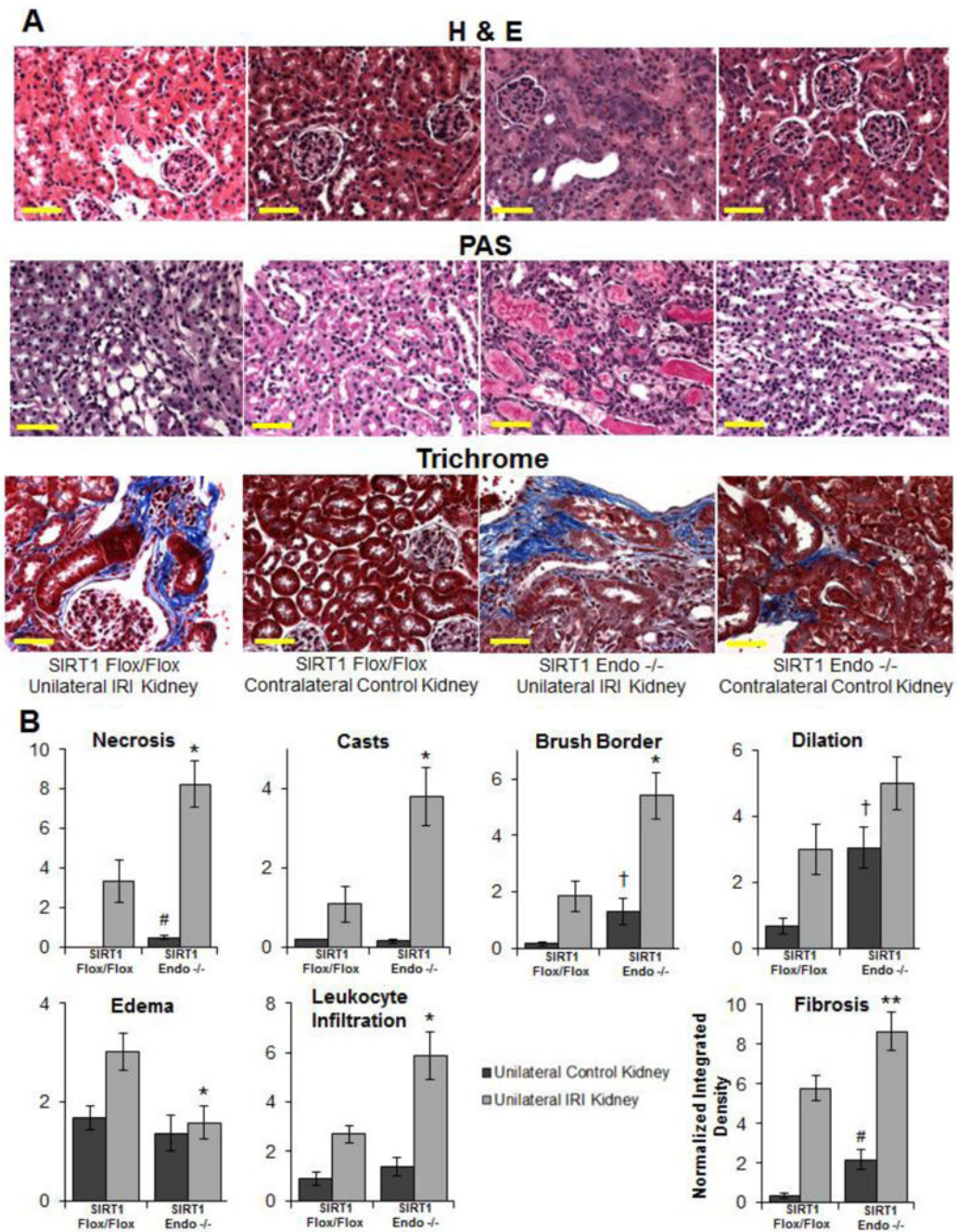


Figure 12. Histological analysis of renal damage in SIRT1 Flox/Flox and SIRT1 endothelial -/- mice 5 days after a 30 minute episode of unilateral renal IRI

SIRT1 endothelial -/- mice exhibited worse renal damage after IRI in both the ischemic and contralateral control kidney, as indicated by hematoxylin and eosin, periodic acid-shift, and Masson's trichrome staining (A). Quantification analyses of pathological damage (B) indicated the ischemic kidney exhibited enhanced necrosis, brush border loss, cast formation, leukocyte infiltration and fibrosis, while the contralateral control kidney in SIRT1 endothelial -/- also demonstrated significant necrosis, brush border loss, tubular dilation and fibrosis. #p<0.05 vs. SIRT1 Flox/Flox control; **p 0.05 vs. SIRT1 Flox/Flox

IRI; † $p < 0.10$ vs. SIRT1 Flox/Flox control; * $p < 0.10$ vs. SIRT1 Flox/Flox IRI; $n = 3$. All images are 400x magnification. Scale bar represents 50 μm .

Author Manuscript

Author Manuscript

Author Manuscript

Author Manuscript